Biotechnology Letters (2005) 27: 1777–1784
DOI 10.1007/s10529-005-3555-2

Rational design of thermostable lactate oxidase by analyzing quaternary structure and prevention of deamidation

Hiroki Kaneko[1,*], Hirotaka Minagawa[2] & Jiro Shimada[2]
[1]*Department of Integrated Sciences in Physics and Biology, College of Humanities and Sciences, Nihon University, 156-8550, Setagaya, Tokyo, Japan*
[2]*Fundamental and Environmental Research Laboratories, NEC Corporation, 305-8501, Tsukuba, Ibaraki, Japan*
**Author for correspondence (Fax: +81-3-5317-9432; E-mail: kaneko@phys.chs.nihon-u.ac.jp)*

Received 26 July 2005; Revisions requested 18 August 2005; Revisions received 6 September 2005; Accepted 7 September 2005

Key words: biosensor, computer-aided design, lactate oxidase, protein engineering, thermostability

Abstract

Our current knowledge of protein unfolding is overwhelmingly related to reversible denaturation. However, to engineer thermostable enzymes for industrial applications and medical diagnostics, it is necessary to consider irreversible denaturation processes and/or the entire quaternary structure. In this study we have used lactate oxidase (LOD), which is employed in lactic acid sensors, as a model example to design thermostable variants by rational design. Twelve mutant proteins were tested and one of them displayed a markedly greater thermostability than all the mutants we had previously obtained by random mutagenesis. This mutant was designed so as to strengthen the interaction between the subunits and stabilize the quaternary structure. Since LOD is difficult to crystallize, its three-dimensional structure remains unknown. This study shows that it is possible to carry out rational design to improve thermostability using a computer-aided quaternary structure model based on the known tertiary structure of a related protein. Critical factors required for increasing the thermal stability of proteins by rational design, where the 3-D structure is not available, are discussed.

Introduction

Protein denaturation consists of reversible and irreversible denaturation. The process is displayed by the following model, that the native protein (N) unfolds into an unfolded state (U), and then reacts further to a denatured state (D) (Petersen *et al.* 2001). However, there are many cases in which plural intermediates (I) exist between N state and U state.

$$N \Leftrightarrow U \rightarrow D$$

Aggregation is a major factor during irreversible denaturation. Another is the cleavage of covalent bonds such as deamidation of asparagine/glutamine residues (Ahern *et al.* 1987). Furthermore, in proteins comprising more than one polypeptide chain, we have to consider inactivation accompanied by dissociation of subunits. If dissociation occurs prior to changes in the structure of each subunit, strengthening of interaction between the subunits is the most important factor in increasing stabilization. It seems that dissociation of subunits occurs at the step of reversible denaturation (Zhou *et al.* 2000) or at the step of irreversible denaturation (Ahern *et al.* 1987). Denaturation, especially irreversible denaturation, is a poorly understood process at the molecular level. There is a paucity of knowledge concerning the irreversible denaturation states and the corresponding 3-D structures. Indeed, there are very few examples in

the literature of successfully increasing the thermostability of an enzyme by rational protein engineering, in which the irreversible denaturation and the dissociation of subunits are considered. However, we cannot avoid these problems in order to enable the industrial use of proteins under severe conditions.

We have attempted to understand the irreversible denaturation and the dissociation of subunits by engineering a thermostable lactate oxidase (LOD). LOD catalyzes the oxidation of lactic acid to give pyruvic acid, with the concomitant reduction of O_2 to H_2O_2 (Sagai *et al.* 1989). LOD is widely used as a lactate biosensor for measuring lactate concentration in body fluids such as blood. It is desirable to improve the thermostability of LOD in order to extend the life of the sensor. We have conducted a series of studies to improve the thermostability of LOD by random mutagenesis (Kaneko *et al.* 1998, Minagawa *et al.* 1998) but, despite considerable effort devoted to solving the 3-D structure of LOD by several groups including our own, the protein has remained recalcitrant to crystallization for X-ray analysis (Morimoto *et al.* 1998). In the absence of structural data, we have deduced the crucial residues for thermostability from the primary amino acid sequence alone. In this paper, the deductive and unusual design for thermostability by using a computer-aided quaternary structure model and stability of LOD mutants actually prepared are reported.

Materials and methods

Homology modeling of lactate oxidase

Although the structure of LOD has not been elucidated, the 3-D structure of spinach-derived glycolate oxidase (GOX), belonging to the same FMN-dependent α-hydroxy acid oxidase family, is known (Lindqvist 1989). We previously predicted the tertiary structure of a subunit of LOD based on homology modeling using a GOX structure as a template (Kaneko *et al.* 1998). However, our studies show that the active LOD enzyme is a homotetramer (data not shown). Therefore, in this study, we predicted a quaternary structure (tetramer structure) based on the crystal structure of GOX (Lindqvist 1989), as shown in Figure 1. Moreover, we performed a detailed analysis to identify amino acid residues which play an important role not only at the active site and coenzyme binding site, but also at the interface between the subunits.

Design of thermostable mutants

Since the purpose of this work was to improve thermostability, we avoided introducing mutations near the active site and coenzyme binding site, which could directly influence enzyme activity, but concentrated on residues located far away from these regions. We adopted the following three strategies as principles for thermostable

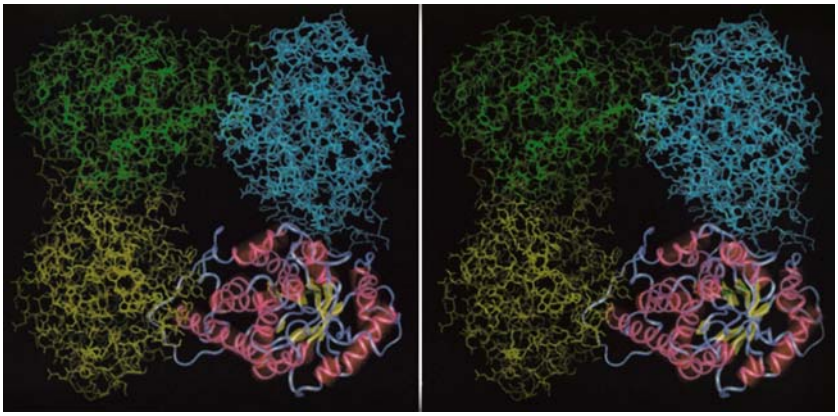

Fig. 1. Quaternary structure of LOD. Only one subunit is displayed by ribbon model. Helix and sheet are illustrated by red cylinder and yellow arrows, respectively. The other three subunits (yellow, green and cyan), both major chains and side chains, are indicated by stick models.

enzyme design which targeted reversible denaturation, irreversible denaturation and stabilization of quaternary structure, respectively. In the first and second strategies, the stability of only one subunit of LOD was considered. Firstly, we attempted to improve the stability of the α-helix itself constructing the $(\beta/\alpha)_8$ barrel structure or the stability among the helices. This is based on the principle that thermostabilization is obtained by decreasing enthalpy of the structure in the N state and consequently increasing the free energy difference between the N state and U state. Secondly, we aimed to decrease asparagine-deamidation at elevated temperature. Lastly, we attempted to strengthen the various intermolecular forces acting between the subunits.

To select the precise location and desired amino acid substitutions that satisfy the above conditions, detailed observation on the quaternary structure model of LOD was carried out by using a 3-D display system. Onyx2 (Silicon Graphics, Inc.) was used as hardware and Discover/Insight II (Accelrys Inc.) was used as display and analysis software.

Preparation of mutants and measurement of thermostability

Mutant LODs were prepared by PCR-based site-directed mutagenesis using the Quick Change Site-Directed Mutagenesis Kit (STRATAGENE) and mutagenic primers (Minagawa *et al.* 1998). The template for the PCR was wild-type LOD gene from *Aerococcus viridans* (gene accession number D50611) cloned into pKK223-3 designated as pLODWt. Forward and reverse primers encoding the required mutations were used to amplify the entire plasmid. The following PCR conditions were used: 95 °C for 30 s, followed by 12 cycles of 95 °C for 30 s, 55 °C for 1 min and 68 °C for 12 min. Template DNA was removed by digestion with *Dpn*I (10 units for 1 h at 37 °C). *E. coli* XL1-Blue was transformed with the reaction mix. Typically we screened 3–5 clones by DNA-sequencing to obtain the desired mutation. Crude cell-free extracts of the mutant clones were prepared by ultrasonication followed by centrifugation (12000×*g*, 20 min, 4 °C). Protein concentration of crude extracts was measured by the BCA protein assay, and diluted to 50 μg/ml. The crude extracts were incubated at various temperatures for 10 min, and then cooled on ice. Residual enzyme activity was measured at room temperature by a peroxidase photometric assay, and thermostability was compared.

Results and discussion

Design for stabilization of $(\beta/\alpha)_8$ barrel structure

LOD is classified in the FMN-dependent α-hydroxy acid oxidase family, which also includes GOX (Lindqvist 1989) and FMN-binding domain of flavocytochrome b_2 (FCB2) (Xia & Mathews 1990). The enzymes belonging to this family have a common $(\beta/\alpha)_8$ barrel structure. The single subunit of LOD probably possesses a $(\beta/\alpha)_8$ barrel structure based on their evident sequence similarity. We previously obtained thermostable mutants of LOD by random mutagenesis (Minagawa *et al.* 1998). The mechanism of stabilization of these mutants was analyzed by comparing the model structure of LOD with the crystal structures of related enzymes (GOX, FCB2). We concluded that strengthening the interactions between two adjacent helices, comprising the $(\beta/\alpha)_8$ barrel structure, stabilized the entire barrel fold and provided thermostability (Kaneko *et al.* 1998).

In this study we examined the eight helices comprising the $(\beta/\alpha)_8$ barrel in GOX and FCB2 in detail. Sites of interaction, such as hydrogen bonds and salt bridges, were identified between the two adjacent helices. The corresponding sites in LOD were then analyzed. Particular attention was given to those sites in LOD that apparently lacked this type of helix interaction. Two sites were found that satisfied these criteria. One site is located between the first (α_1) and second helix (α_2), which comprises the $(\beta/\alpha)_8$ barrel (Figure 2). The α_2 helix contains glutamic acid residues, which are conserved among three proteins (residue 131 of LOD; 115 of GOX; 237 of FMN-binding domain of FCB2). In both GOX and FCB2, these glutamate residues form hydrogen bonds with amino acids located in the α_1 helix (Tyr90 and Lys210, respectively). However, the corresponding site in the α_1 helix of LOD is Ala106, which does not interact with the glutamate residue located in the α_2 helix. In order to strengthen the interaction between the α_1 and α_2 helices in LOD, we designed mutants in which

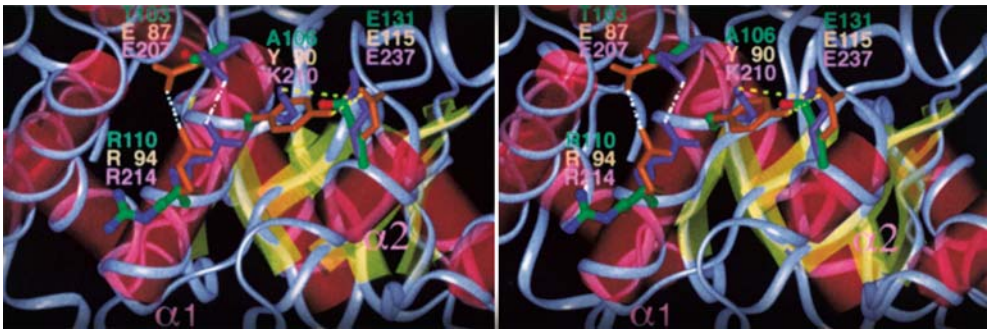

Fig. 2. Peripheral environment of helix α_1 and helix α_2 of LOD and related enzymes. Side chains of LOD are displayed by colored stick in each atom (carbon, green; nitrogen, blue; oxygen, red). The individual side chains of GOX and FMN-binding domain of flavocytochrome b_2 (FCB2) are colored orange and purple, respectively. The number of residues, LOD, GOX and flavocytochrome b_2 correspond to upper row (green), middle row (orange) and lower row (purple). Yellow dotted line and white dotted line indicate the hydrogen bond between α_1 helix and α_2 helix, and hydrogen bond insides the α_1 helix, respectively. Red cylinder and yellow arrow represent helices and sheets, respectively.

Ala106 was substituted with Tyr (as for GOX) or Lys (as for FCB2**).** The second site in LOD that matched our criteria was located between the α_7 and α_8 helices. Here again, the site of interaction found in the GOX and FCB2 family of proteins was absent in LOD. Accordingly, we designed a mutant in which Asp344 was substituted with Glu.

When only the α_1 helix in both GOX and FCB2 were studied in isolation, an interaction between two side chains was observed in the same helix **(**Figure 2**).** Specifically these are between Glu87 and Arg94 in GOX, and between Glu207 and Arg214 in the FMN-binding domain of FCB2. However, only the Arg residue is conserved at the corresponding sites in LOD (Thr103 and Arg110). Therefore, in order to stabilize the α_1 helix, we designed a mutant in which Thr103 was substituted by Glu. The same rationale was used to identify a second site in the α_8 helix of LOD. We therefore designed a second mutation (Trp331 to Glu) to enhance the stability of the α_8 helix.

Design by considering irreversible denaturation (prevention of deamidation of asparagine/ glutamine)

One of factors in the irreversible denaturation is the potential deamidation of asparagine and glutamine residues. Deamidation of asparagine residues has a marked effect on the surrounding electrostatic field by generating a negative charge (i.e. aspartic acid). Indeed, the thermostability of triose-phosphate isomerase was markedly increased by substituting Asn residues, located at the interfacial boundary of the subunit domains, with Thr or Ile in order to prevent deamidation-driven dissociation of the active dimer (Ahern *et al.* 1987).

We carefully examined the model structure of LOD, but could not find Asn or Gln at the interface of the subunits. Instead, we discovered Asn154, which is slightly buried in the interior and surrounded by a constellation of negatively charged residues (Figure 3). We predicted that when this asparagine is deamidated, electrostatic repulsion with the outlying residues would significantly weaken the packing. Therefore, we designed a mutant in which Asn154 was substituted with either Thr or Ile.

Design for stabilization of quaternary structure

The quaternary structure of GOX (Lindqvist 1989) was predicted to have the greatest similarity to LOD. We studied the interactions between the subunits of GOX in detail. We noticed that Leu52 of one subunit was almost buried in a hydrophobic pocket (comprised of Leu154, Val156, Trp213, Val216, Ile227 and Val229) of the juxtaposed subunit. When this region was inspected using the tetramer model of LOD (Figure 1), a similar hydrophobic pocket was predicted. Leu52 of GOX corresponded to Ala68 in the predicted structure of LOD. However the model structure

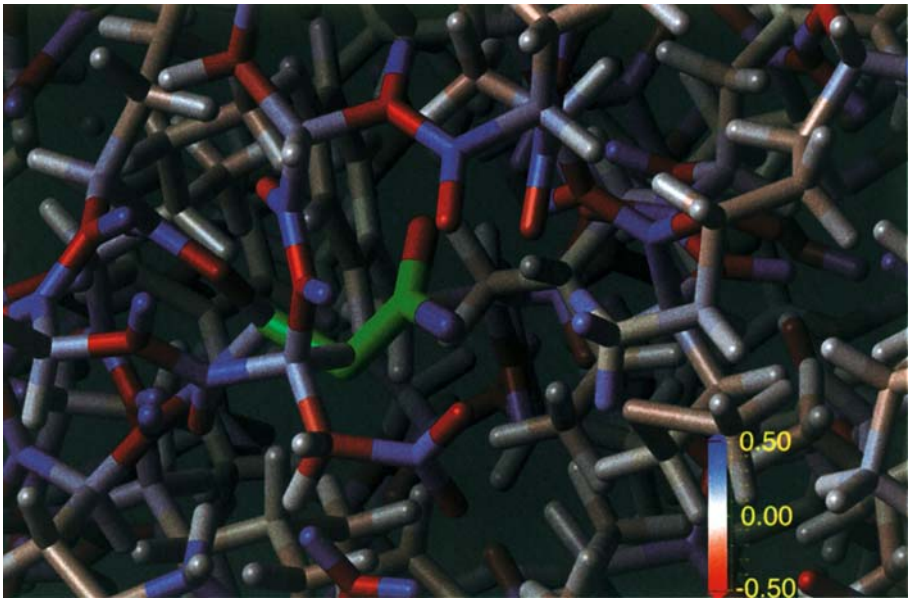

Fig. 3. Electrostatic environment around Asn 154 of LOD. Asn 154 is illustrated by a colored stick in each atom (carbon, green; nitrogen, blue; oxygen, red). Other portions were colored dependent on the values of point charges distributed to each atom. The portion colored by darker red shows stronger minus charge.

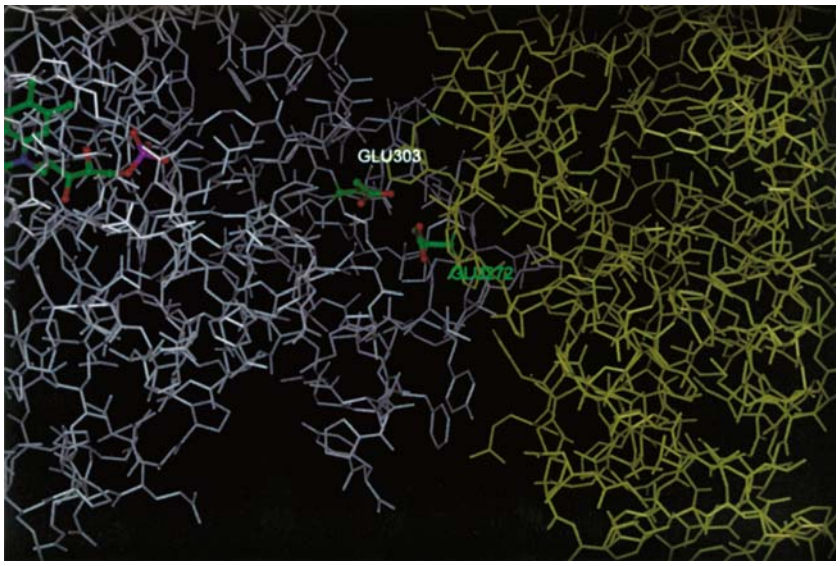

Fig. 4. Interaction between subunit 1 and subunit 2 in the LOD model. Subunit 1 and 2 are respectively shown by silver and yellow sticks. Glu303 in subunit 1, Glu272 in subunit 2 and FMN in subunit 1 are indicated by atom-type color.

indicated that, because of the shorter side chain, the Ala residue cannot fit into the hydrophobic pocket of the adjoining subunit. Therefore, we designed an Ala68 to Val or Leu mutant in order to strengthen the hydrophobic interactions at the subunit interface. Another important point of contact between the subunits of GOX involves the cluster of hydrophobic residues Phe47, Leu336 and Leu340 which interact with Leu259 on the adjacent subunit. The amino acids of LOD that

Table 1. Mutant LODs designed by using computer-aided model.

Position	Mutation	Meaning of mutation
68	Ala → Val	Stabilization of tetramer by strengthening hydrophobic interaction among subunits
68	Ala → Leu	Stabilization of tetramer by strengthening hydrophobic interaction among subunits
103	Thr → Glu	Stabilization of α_1 helix
106	Ala → Tyr	Strengthening interaction between α_1 helix and α_2 helix
106	Ala → Lys	Strengthening interaction between α_1 helix and α_2 helix
154	Asn → Thr	Prevention of deamidation of asparagine residue
154	Asn → Ile	Prevention of deamidation of asparagine residue
272	Glu → Gln	Stabilization of tetramer by removing electrostatic repulsion among subunits
303	Glu → Gln	Stabilization of tetramer by removing electrostatic repulsion among subunits
331	Trp → Glu	Stabilization of α_8 helix
344	Asp → Glu	Strengthening interaction between α_7 helix and α_8 helix
347	Arg f → Leu	Stabilization of tetramer by strengthening hydrophobic interaction among subunits

correspond to the four hydrophobic residues were Leu63, Arg347, Leu351 and Leu270. Clearly Arg347 will weaken any hydrophobic interaction at the subunit interface. Therefore, we designed the mutant Arg347 to Leu.

Interestingly, we discovered a site in LOD that is thought to weaken the interaction among the subunits. The corresponding site was absent in GOX. The site in LOD comprises two residues, Glu272 and Glu303, which are juxtaposed at the interface of each subunit and have the potential for electrostatic repulsion (Figure 4). Therefore, we designed mutants in which one of the residues was substituted with Gln (i.e. Glu272 to Gln or Glu303 to Gln) in order to prevent dissociation of the subunits and strengthen the interaction by hydrogen bonding.

Table 1 summarizes all 12 mutant types based on the rationale outlined in the above three sections (i.e. design for stabilization of $(\beta/\alpha)_8$ barrel structure, design by considering irreversible denaturation and design for stabilization of quaternary structure).

Thermostability of mutants

We engineered the designed mutants and measured enzyme activity of crude extracts from each individual variant. Results are shown in Table 2. For comparison, we added data from mutant E160G, which had been obtained by random mutagenesis in our previous study (Minagawa *et al.* 1998). In the past we have analyzed the thermostability of LOD mutants using both crude extracts and purified enzymes, and confirmed that the two methodologies were wholly consistent. Therefore, although the results in this study were obtained using crude extracts, the relative changes in thermostability accurately reflect the characteristics of the mutant enzymes. Moreover, in the heating experiment on wild-type enzyme performed at 70 °C for 10 min, the enzyme exhibited no restoration of the lost activity. In this respect, it is assumed that all the data in Table 2, which is obtained at almost 70 °C, is highly relevant to irreversible denaturation as the case of the wild-type.

We deliberately chose to mutate residues located far away from the active site so as not to influence enzyme activity. Nevertheless, mutants E272Q and W331E lost almost all enzyme activity. It is difficult to understand precisely why a single amino acid substitution, distant from the active site, should result in such a large loss of activity. We conclude that the whole folding structure was made unstable by the amino acid substitutions and consequently the strict side chains arrangements of active site residues was disordered. The thermostability of other mutants except these two mutants is discussed below.

The mutants designed to have a stabilized $(\beta/\alpha)_8$ barrel structure (T103E, A106Y, A106K, D344E), showed the same or lower thermostability, as compared to wild-type. In particular A106Y, A106K and D344E displayed poor thermostability, despite the introduction of hydrogen bonds or salt bridges intended to enhance the interaction between the two helices comprising

Table 2. Thermal inactivation of wild-type and mutant.

Mutation	Initial activity[a]	60 °C 10 min[b]	65 °C 10 min[b]	70 °C 10 min[b]	75 °C 10 min[b]
A68V	93	75 ± 1.28	19 ± 0.79	0 ± 0	0 ± 0
A68L	91	112 ± 10.3	51 ± 4.68	0 ± 0	0 ± 0
T103E	22	61 ± 12.1	0 ± 0	0 ± 0	0 ± 0
A106Y	83	86 ± 1.53	52 ± 2.69	0 ± 0	0 ± 0
A106K	72	65 ± 4.78	45 ± 3.3	0.3 ± 0.2	0 ± 0
N154T	83	78 ± 7.16	42 ± 10.3	0 ± 0	0 ± 0
N154I	10	30 ± 2.75	44 ± 8.76	0 ± 0	0 ± 0
E272Q	0	0 ± 0	0 ± 0	0 ± 0	0 ± 0
E303Q	6	108 ± 12.2	93 ± 8.5	17 ± 1.56	0 ± 0
W331E	0	0 ± 0	0 ± 0	0 ± 0	0 ± 0
D344E	48	68 ± 6.76	29 ± 2.66	0 ± 0	0 ± 0
R347L	40	93 ± 3.89	30 ± 5.97	0 ± 0	0 ± 0
Wild type	100	78 ± 1.39	57 ± 2.39	0 ± 0	0 ± 0
E160G	41	84 ± 7.71	72 ± 5.3	12 ± 2.39	0 ± 0

Protein concentration of crude enzyme was adjusted to 50 μg/ml. Results represent the mean value of experiments performed in triplicate ± SD.
[a]Relative activity of mutant LODs at room temperature are expressed as a percentage of wild-type activity.
[b]Remaining activity of wild-type and mutant LODs are expressed as a percentage of initial activity.

the barrel structure in order to imitate other members of family protein. It is possible that the bulkier side chains, for introducing hydrogen bonds and salt bridges, caused steric hindrance with nearby residues. Even if there were any decrease in enthalpy of the natural state and any increase in $\Delta G_{N \Leftrightarrow U}$ caused by stabilization of the $(\beta/\alpha)_8$ barrel structure, these affected the reversible denaturation process, which occurs at relatively low temperature. Therefore, it is thought that irreversible denaturation shown in Table 2 was neither influenced nor reflected in the data.

The mutants designed for prevention of deamidation (N154T and N154I) did not show increased thermostability over the wild-type enzyme. The following factors must be considered: (i) stabilization of LOD was barely influenced even if deamidation of Asn154 occurs, (ii) heating at 75 °C was not sufficient to cause deamidation, which is a factor in irreversible denaturation (at ~100 °C).

Of the mutants designed for stabilization of quaternary structure (A68V, A68L, E303Q and R347L), only E303Q showed a greater thermostability than E160G, which was the best mutant obtained by random mutagenesis (Minagawa *et al.* 1998). However, the initial enzyme activity of E303Q prior to heat treatment (relative activity as a percentage of wild-type: 6%) was low in comparison to that of wild-type enzyme (100%). Although this mutant has a serious problem with the practical use due to kinetic factors, the increased thermostability obtained by this approach is nevertheless of great interest. Strengthening interactions between subunits and stabilizing the entire quaternary structure by rational design resulted in a greater improvement in thermostability than mutants obtained by screening several tens of thousands of mutants produced by random mutagenesis. Moreover, it is significant that protein design based on structural information from a related enzyme can be accomplished using a computer-aided model of quaternary structure.

Why did so many mutants show only a slight improvement in thermostability, contrary to our expectations? One reason might be the accuracy of the LOD model. Given the high level of sequence homology between GOX and LOD (~35 % identity), we are confident that the secondary structure predictions of the barrel and the main chain are valid. However, fine structural details of the side chains are uncertain, even though energy optimization and molecular dynamic calculations were rigorously performed. Knowledge of the precise orientation of the side chains is therefore critical in designing thermostable proteins from a model structure. There are no specific design rules for preventing irreversible denaturation, which differ from those for reversible denaturation

(e.g. cross-linking by S−S bond (Matsumura *et al.* 1989a,b), strengthening of hydrophobic core (Yutani *et al.* 1987, Matsumura *et al.* 1988) and reinforcement of main chains by Pro (Matthews *et al.* 1987, Nicholson *et al.* 1992)). In this study, we have actively explored ways of preventing irreversible denaturation by reducing deamidation of asparagine and by strengthening interaction between subunits. It is important to elucidate the factors causing irreversible denaturation from the physicochemical properties of the protein. In future we intend to incorporate these factors into the theoretical design model for protein engineering.

References

Ahern TJ, Casal JI, Petsko GA, Klibanov AM (1987) Control of oligomeric enzyme thermostability by protein engineering. *Proc. Natl. Acad. Sci. U/S.A.* **84**: 675−679.

Kaneko H, Minagawa H, Nakayama N, Nakamoto S, Handa S, Shimada J, Takada T, Umeyama H (1998) Modeling study of a lactate oxidase-ligand complex: Substrate specificity and thermostability . *Res. Commun. Biochem. Cell Mol. Biol.* **2**: 234−244.

Lindqvist Y (1989) Refined structure of spinach glycolate oxidase at 2 Å resolution. *J. Mol. Biol.* **209**: 151−166.

Matsumura M, Becktel WJ, Matthews BW (1988) Hydrophobic stabilization in T4 lysozyme determined directly by multiple substitutions of Ile 3. *Nature* **334**: 406−410.

Matsumura M, Becktel WJ, Levitt M, Matthews BW (1989a) Stabilization of phage T4 lysozyme by engineered disulfide bonds. *Proc. Natl. Acad. Sci. U.S.A.* **86**: 6562−6566.

Matsumura M, Signor G, Matthews BW (1989b) Substantial increase of protein stability by multiple disulphide bonds. *Nature* **342**: 291−293.

Matthews BW, Nicholson H, Becktel WJ (1987) Enhanced protein thermostability from site-directed mutations that decrease the entropy of unfolding. *Proc. Natl. Acad. Sci. U.S.A.* **84**: 6663−6667.

Minagawa H, Nakayama N, Nakamoto S, Kaneko H (1998) Lactate oxidase thermostabilized by random mutagenesis. *Res. Commun. Biochem. Cell Mol. Biol.* **2**: 149−156.

Morimoto Y, Yorita K, Aki K, Misaki H, Massey V (1998) L-lactate oxidase from *Aerococcus viridans* crystallized as an octamer. Preliminary X-ray studies. *Biochimie* **80**: 309−312.

Nicholson H, Tronrud DE, Becktel WJ, Matthews BW (1992) Analysis of the effectiveness of proline substitutions and glycine replacements in increasing the stability of phage T4 lysozyme. *Biopolymers* **32**: 1431−1441.

Petersen SB, Fojan P, Petersen EI, Petersen M (2001) The thermal stability of the *Fusarium solani pisi* cutinase as a function of pH. *J. Biomed. Biotechnol.* **1**: 62−69.

Sagai H, Nagata K, Misaki, H (1989) Toyo Jozo Co., Ltd. European Patent. EP 0376163 A2.

Xia ZX, Mathews FS (1990) Molecular structure of flavocytochrome *b2* at 2.4 Å resolution. *J. Mol. Biol.* **212**: 837−863.

Yutani K, Ogasahara K, Tsujita T, Sugino Y (1987) Dependence of conformational stability on hydrophobicity of the amino acid residue in a series of variant proteins substituted at a unique position of tryptophan synthase alpha subunit. *Proc. Natl. Acad. Sci. U.S.A.* **84**: 4441−4444.

Zhou J-M, Zhu L, Balny C (2000) Inactivation of creatine kinase by high pressure may precede dimer dissociation. *Eur. J. Biochem.* **267**: 1247−1253.